Gating of Local Network Signals Appears as Stimulus-Dependent Activity Envelopes in Striate Cortex

N. D. SCHIFF, K. P. PURPURA, AND J. D. VICTOR
Department of Neurology and Neuroscience, Joan and Sanford I. Weill Medical College of Cornell University, New York, New York 10021

Schiff, N. D., K. P. Purpura, and J. D. Victor. Gating of local network signals appears as stimulus-dependent activity envelopes in striate cortex. *J. Neurophysiol.* 82: 2182–2196, 1999. Neuronal activity often is treated as a composition of a stimulus-driven component and a second component that corrupts the signal, adding or deleting spikes at random. Standard quantitative methods such as peristimulus histograms and Fourier analysis use stimulus-locked averaging to enhance detection of the driven component of neuronal responses and de-emphasize the "noise." However, neural activity also includes bursts, oscillations, and other episodic events that standard averaging methods overlook. If this activity is stimulus independent, it can be characterized by standard power spectral analysis (or autocorrelation). But activity that is excited by (but not temporally locked to) the visual stimulus cannot be characterized by averaging or standard spectral analysis. Phase-locked spectral analysis (PLSA) is a new method that examines this "residual" activity—the difference between the individual responses to each cycle of a periodic stimulus and their average. With PLSA, residual activity is characterized in terms of temporal envelopes and their carriers. Previously, PLSA demonstrated broadband interactions between periodic visual stimuli and fluctuations in the local field potential of macaque V1. In the present study, single-unit responses (SUA) from parafoveal V1 in anesthetized macaque monkey are examined with this technique. Recordings were made from 21 neurons, 6 of which were recorded in pairs along with multiunit activity (MUA) from separate electrodes and 8 of which were recorded along with MUA from the same electrode. PLSA was applied to responses to preferred (orientation, direction, and spatial frequency) and nonpreferred drifting gratings. For preferred stimuli, all cells demonstrated broadband (1–10 Hz and higher) residual activity that waxed and waned with the stimulus cycle, suggesting that changes in the residual activity are introduced routinely by visual stimulation. Moreover, some reconstructed envelopes indicate that the residual activity was sharply gated by the stimulus cycle. Oscillations occasionally were seen in the power spectrum of single units. Phase-locked cross-spectra were determined for 3 SUA/SUA pairs and 11 SUA/MUA pairs. Residual activity in the cross-spectra was generally much less than the residual activity determined separately from each neuron. The reduction in the residual activity in the cross-spectra suggests that nearby neurons may gate inputs from distinct and relatively independent neuronal subpopulations that together generate the background rhythms of striate cortex.

INTRODUCTION

The issue of what constitutes "signal" and what constitutes "noise" is present at all levels of investigation of neuronal activity, from single (SUA)- and multiunit (MUA)

recordings to recordings of local (LFP) and far field (ECoG, EEG) potentials. The usual approach in neurophysiological investigations is to equate signal with the "average response"—whatever is reinforced with peristimulus averaging of Fourier analysis. Variations of individual responses from this average response necessarily are eliminated. This residual activity may include oscillations, bursts, and changes in the variability of firing rate (mean-variance relationship) (Gershon et al. 1998).

At present, considerable attention has been given to oscillations in both LFP and SUA/MUA recordings as an example of the type of temporal structure in the noise of neuronal responses (Freeman and Barrie 1994; Singer and Gray 1995). However, as Bullock (1996) recently noted, spectral analysis of brain activity typically does not reveal narrow peaks suggestive of independent oscillators. Other types of episodic dynamics, such as bursts (Lisman 1997), transient responses (Friston 1995; Victor and Purpura 1996), stereotypical patterns of intervals (Abeles 1988), and maintained elevated discharges (Moran and Desimone 1995; Treue and Maunsell 1996), may be more representative of ongoing brain activity. It is crucial not only to demonstrate the existence of such phenomena in residual fluctuations but also to define their relationship to external stimuli.

Examination and quantification of such episodic events in the context of their possible roles in information coding and processing requires appropriate tools. We present a method, phase-locked spectral analysis (PLSA), that investigates the relationship of average and residual components of neuronal responses and apply it to recordings from macaque primary visual cortex (V1). This method is a natural generalization of the standard Fourier methods used in the calculation of power spectra and can be applied to both field potential and spike train data. Previous studies of the LFP in macaque V1 using PLSA showed evidence of interaction of average activity with the ongoing LFP in the form of such residual components (Victor et al. 1993). Here we examine SUA and MUA recordings from macaque V1 for evidence of such changes in residual activity. The analysis demonstrates an interaction of periodic stimulation and residual activity that is typically broadband. We also examine interaction of neurons in paired SUA/MUA and SUA/SUA recordings. Our results demonstrate that stimulus-induced changes in the residual activity of one cell are correlated only weakly with such changes in nearby cells. This implies that residual cortical activity reflects multiple, relatively independent, cell assemblies.

METHODS

Phase-locked spectral analysis

PLSA is a natural extension of spectral analysis to situations in which a periodic stimulus is present, and its possible influence on residual activity is of interest. In analogy with the standard power spectrum (see *Eq. A16*), we define the phase-locked spectrum of order n at the frequency ω by

$$P_n(\omega) = \lim_{L \to \infty} L X_{av}\left(\frac{\pi n}{S} - \omega, \frac{\pi n}{S} + \omega, L, 0\right) \qquad (1)$$

Where S is the stimulus period, L is the analysis period, and X_{av} is a covariance of Fourier components at the frequencies $\omega - (\pi n/S)$ and $\omega + (\pi n/S)$ (see APPENDIX). $P_n(\omega)$ has units of (impulse/s)^2/Hz, or equivalently, seconds^{-1}.

Interpretation of PLSA in terms of envelope and carrier

A nonzero value for $P_n(\omega)$ implies that the joint appearance of components at these frequencies is more likely than expected from their individual representation in the power spectrum. When n/S is small compared with ω, the joint appearance of these frequencies can be interpreted as a "beat" with carrier frequency ω and envelope period S/n. That is, $P_n(\omega)$, for each n, describes the power at the frequency ω that varies with the nth harmonic of the external stimulus. Note that $P_n(\omega)$ is a complex-valued quantity. Its amplitude and phase are the amplitude and phase of the beat's *envelope*. We emphasize that the phase of the *carrier* has no preferred value with respect to the stimulus cycle because such a preferred phase would have contributed to the average response, which was subtracted out (see *Eq. A9*).

Figure 1, *A–D*, illustrates several time series the statistics of which are revealed by PLSA. In all cases, the average over the stimulus cycle is a sinusoid the period of which is that of the periodic stimulus, S. The *top line* of Fig. 1A illustrates a signal containing variability that
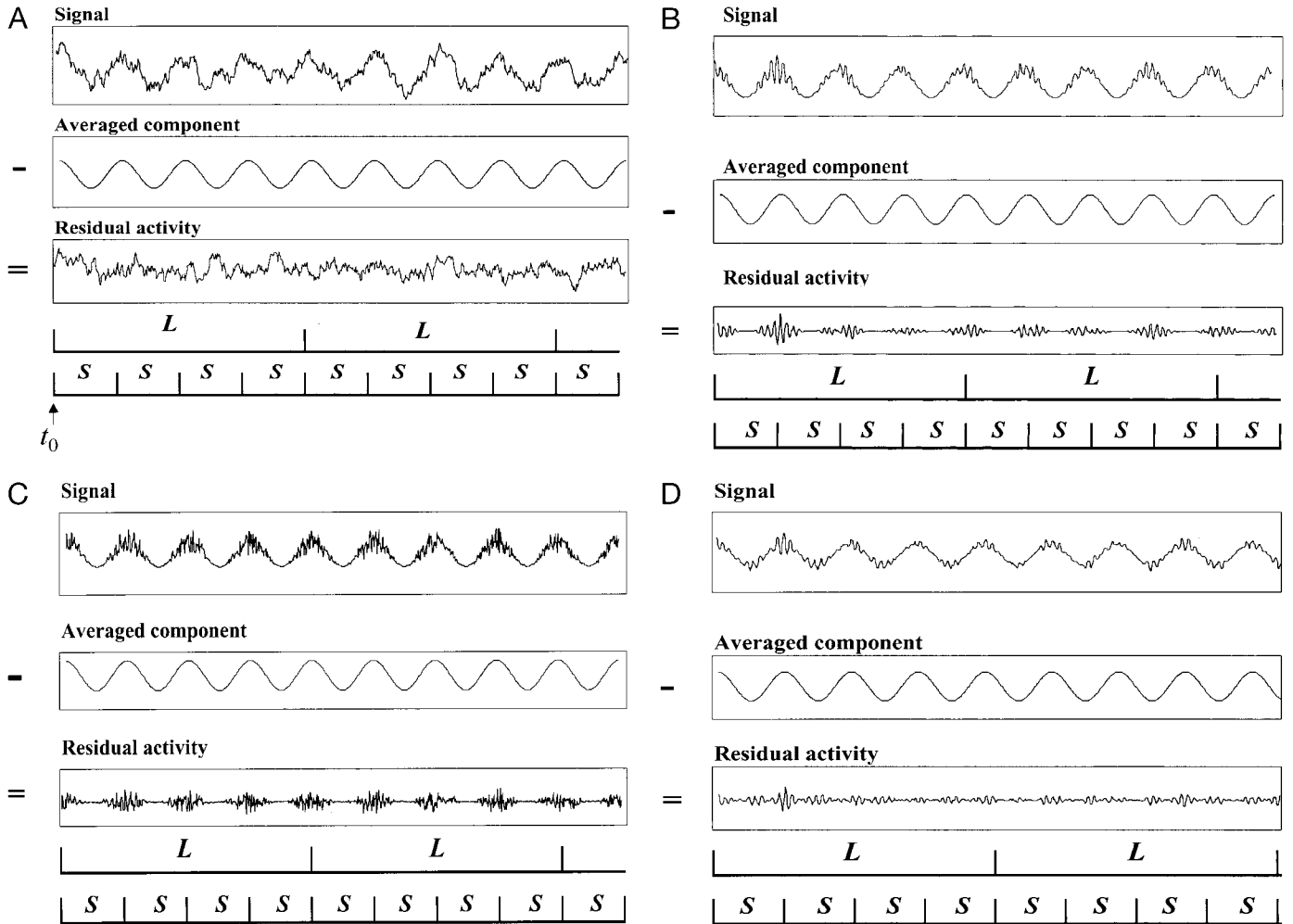

FIG. 1. Diagram of analysis of residual activity. *A*: for standard spectral estimation, a signal *s* is divided into segments of equal length *L*. Arrow marked t_0 indicates the starting time for beginning the calculation. Signal *s* is a sinusoid added to filtered Gaussian noise that is *independent of* the stimulus cycle. Subtraction of the averaged (sinusoidal) component recovers the noise (residual activity). *S* indicates the stimulus cycle. *L,* the analysis period, must be an integer multiple of *S. B*: signal is a sinusoid added to a narrowband noise that waxes and wanes with the *first harmonic* of the stimulus cycle. Subtraction of the averaged (sinusoidal) component reveals this residual activity. Because the residual activity covaries with the first harmonic of the stimulus period *S,* it generates a contribution to the first-order phase-locked spectrum $P_1(\omega)$. *C*: signal is a sinusoid added to a broadband noise that waxes and wanes with the *first harmonic* of the stimulus cycle. As in *B,* the residual activity contributes to the phase-locked spectrum $P_1(\omega)$. *D*: signal is a sinusoid added to a narrowband noise that waxes and wanes with the *second harmonic* of the stimulus cycle. Residual activity, revealed by subtraction of the averaged (sinusoidal) response, contributes to $P_2(\omega)$.

is independent of the stimulus. Subtraction of the period-averaged signal (*2nd line*) reveals a broadband noise (*3rd line*) the statistics of which are independent of the stimulus. For this situation, $P_0(\omega)$ is the spectrum of this broadband noise, and $P_n(\omega)$ ($n > 0$) is zero, indicating the lack of modulation of the residual activity at the frequency of the stimulus or any of its harmonics. The *top line* of Fig. 1*B* illustrates a signal containing variability that waxes and wanes at the first harmonic of the stimulus frequency. This kind of variability is consistent with the mean-variance relationship seen in visual cortical neurons (Gershon et al. 1998; Tolhurst et al. 1983) (see DISCUSSION). The period-averaged signal (*2nd line* of Fig. 1*B*) is sinusoidal as in Fig. 1*A*. However, subtraction of this average yields (*3rd line* of Fig. 1*B*) residual activity that peaks at the start of each stimulus cycle. $P_1(\omega)$ is thus nonzero, indicating that the residual activity (noise) is modulated at the first harmonic of the stimulus frequency. $P_0(\omega)$ is also nonzero and represents the average spectrum of this noise. However, $P_n(\omega)$ ($n > 1$) is zero, indicating the lack of modulation of the noise at higher harmonics of the stimulus frequency. Figure 1*C* is similar to Fig. 1*B*, except that the residual activity is broadband rather than narrowband. As in Fig. 1*B*, $P_0(\omega)$ and $P_1(\omega)$ are nonzero, but their dependence on ω is different, reflecting the different spectral distribution of the noise. Figure 1*D*, like Fig. 1*B*, is an example of a signal containing modulated narrowband residual activity. But in contrast to Fig. 1*B*, there are two noise bursts per stimulus cycle. Thus $P_0(\omega)$ and $P_2(\omega)$ are nonzero and the remaining $P_n(\omega)$ are zero.

Significance testing

We use two approaches to determine whether experimentally measured values of the phase-locked spectra $P_n(\omega)$ (for $n > 0$) are significantly different from zero. One approach is to compare empirically estimated values of $P_n(\omega)$ when a periodic stimulus is present with estimates obtained when the periodic stimulus is removed (i.e., blank screen) and the "true" value of $P_n(\omega)$ is guaranteed to be zero. The second approach makes use of the interpretation of $P_n(\omega)$ in terms of an envelope frequency $2\pi n/S$ and a carrier frequency ω. If $P_n(\omega)$ reflects power in some frequency range around ω that systematically varies at the envelope frequency $2\pi n/S$, then the phases of $P_n(\omega)$ should be coherent across a range of carrier frequencies ω and should reflect the phase of the common envelope. To assess phase coherence, we used the Rayleigh phase criterion (RPC) across bands of frequencies ω (Mardia 1972).

General physiological methods

We recorded single-unit activity in the parafoveal representation in cortical area V1 of six anesthetized, paralyzed macaque monkeys. Twenty-one single units were isolated and stable recordings maintained for sufficient time (2–3 h) for the studies reported here. Other studies were performed on additional cells in these animals (Victor and Purpura 1996, 1998). All procedures involving the animals were performed in accordance with National Institutes of Health guidelines for the care and use of laboratory animals. General physiological preparations, methods, and recording techniques are described elsewhere (Victor and Purpura 1998; Victor et al. 1994).

In 15 recordings, units were isolated from one electrode using criteria implemented by a Tucker-Davis hoop discriminator. In three recordings (6 cells), recordings were made from separate microelectrodes, independently manipulated and laterally displaced by 2 mm. These six single units were recorded as part of pair recordings, along with discrete MUA that could be separated from the single unit but not resolved into individual unit activity. We classified cells as simple or complex by standard Fourier analysis of their responses to drifting gratings and the criteria of Skottun et al.(1991).

For measurement of phase-locked spectra, drifting gratings at a temporal frequency of 1.06 Hz, 100% contrast [$(L_{max} - L_{min})/(L_{max} + L_{min})$] unless otherwise noted, optimal orientation, direction, and spatial frequency were presented to each cell (mean luminance of the computer-

driven CRT display 150 cd/m^2 with a green phosphor, subtending $4 \times 4°$ at a viewing distance of 114 cm). For most cells (see following text), a second grating stimulus and/or a blank was presented in interleaved runs.

Orientation experiment

For six cells, stimuli were interleaved with drifting gratings at the orthogonal orientation but optimal spatial frequency as well as a blank condition. Eight additional cells were studied with two (interleaved) orientations but without the blank condition. Here and in the following text, optimal indicates a maximal fundamental response for simple cells and a maximum elevation of the mean rate for complex cells.

Spatial frequency experiment

For three cells, stimuli were interleaved with drifting gratings at a nonoptimal spatial frequency and a blank condition. The nonoptimal spatial frequency differed from the optimal spatial frequency by at least an octave, and both gratings were presented at the optimal orientation and direction. Ten additional cells were studied with two (interleaved) spatial frequencies but without the blank condition.

Data collection and analysis

Data were collected in continuous streams of 1 min per condition. Thirty-two examples of each condition were interleaved, with ~20 s of uniform illumination at the mean stimulus luminance between runs. Spike times were recorded at the resolution of the frame interval of the display (3.7-ms bins). Responses from each stimulus presentation were segmented into analysis periods of length $L = 3.79$ s (1,024 bins); the stimulus period S was 0.947 s (256 bins). Spikes were considered to be delta-functions, and Fourier estimates (at frequencies <122) $= 2\pi n/L$ were calculated following detrending and windowing with a raised cosine function. By choosing an analysis period that is four times the length of the sampling period ($L = 4S$) and using the raised cosine bell window, spurious correlations due to the leakage of the spectral estimates away from their nominal frequencies are eliminated. Consecutive analysis segments overlapped by half their length to compensate for the effects of windowing (Blackman and Tukey 1959). Rayleigh phase criterion (RPC) calculations (Mardia 1972) were based on nine adjacent frequencies separated by $1/L = 0.26$ Hz, thus spanning a 2-Hz range.

RESULTS

Analysis of single-unit data

Figure 2 displays the analysis of residual activity obtained from a simple cell in macaque V1. The stimuli consisted of drifting gratings at preferred and orthogonal orientations. The peristimulus time histogram (PSTH) of responses to drifting gratings of preferred, orthogonal, and blank runs (Fig. 2*A*) demonstrates a maintained discharge in the "blank" condition, and both modulation and elevation for the preferred orientation. Figure 2*B* shows the zeroth-order phase-locked spectrum, $P_0(\omega)$ in the three conditions. If the stimulus merely influenced neuronal activity by adding a periodic signal to an autonomous noise, $P_0(\omega)$ would be the same in all conditions. However, as shown in Fig. 2*B*, $P_0(\omega)$ is threefold larger for the preferred grating (*top*) than for the nonpreferred grating or the blank stimulus. This difference in power is present over the entire frequency range examined (with a greater difference at frequencies <50 Hz), thus indicating broadband residual activity.

$P_1(\omega)$ (Fig. 2*C*) describes the components of the residual activity that are modulated at the first harmonic of the stimulus
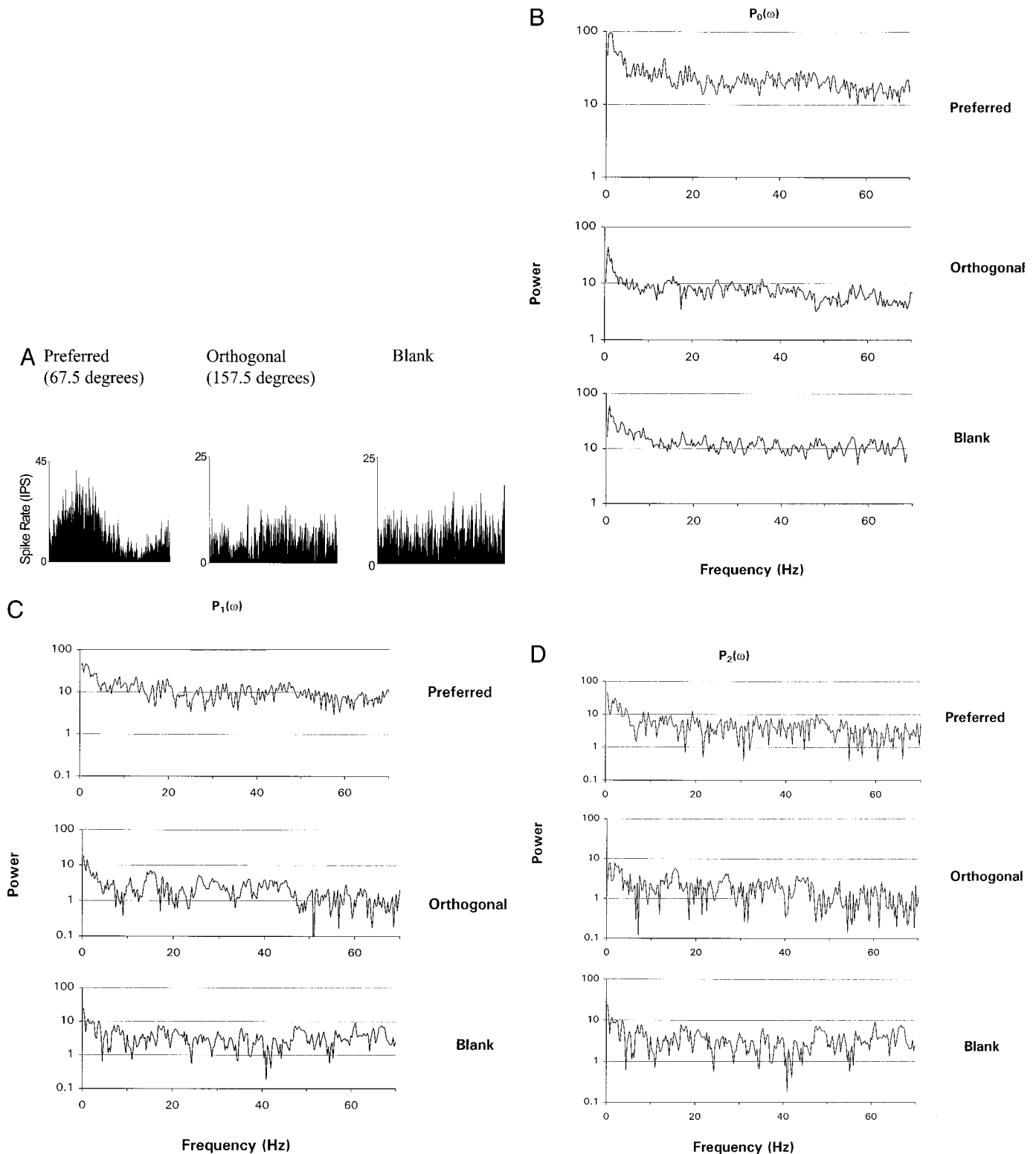
FIG. 2. *A*: peristimulus histograms of a V1 simple cell's response to drifting gratings with orientations of 67.5° (preferred) and 157.5° (orthogonal), presented with a spatial frequency of 2 cycles/°, a temporal frequency of 1.06 Hz, and 100% contrast, and a blank condition (0% contrast). Horizontal scale is one stimulus cycle (1.06 s). Note that there is a significant modulated elevation of the background discharge at the preferred orientation; a maintained discharge is present for the orthogonal and blank conditions. *B*: power spectrum $P_0(\omega)$, corrected for the driven response as described in the text. *C*: amplitude of the first-order phase-locked spectrum $P_1(\omega)$. As described in the text, this is the component of the power that covaries with the first harmonic of the stimulus cycle. *D*: amplitude of the second-order phase-locked spectrum $P_2(\omega)$, which is the component of the power that covaries with the second harmonic of the stimulus cycle. Here and in the following figures, units for amplitudes of $P_n(\omega)$ are (impulses/s)^2/Hz.
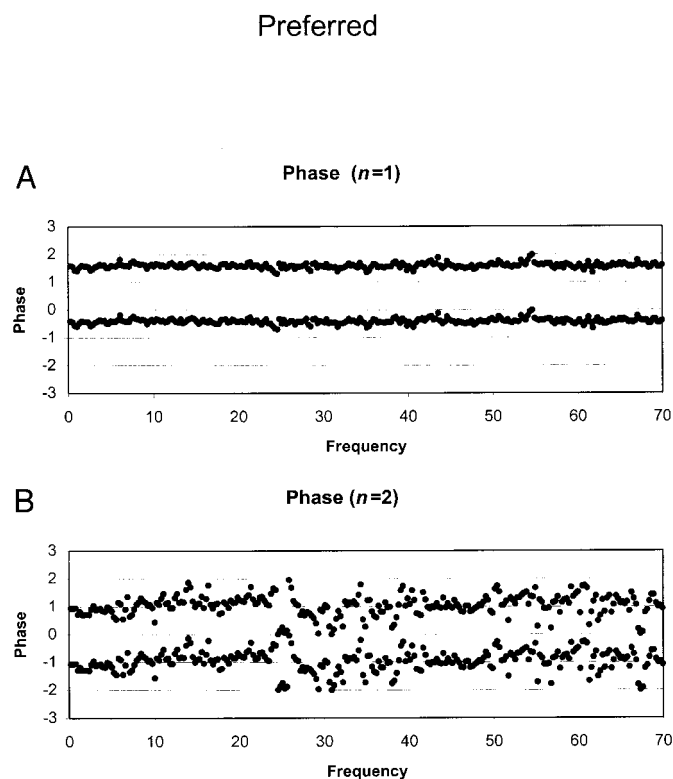
Preferred

A

Phase (n=1)

B

Phase (n=2)

FIG. 3. Phases of the phase-locked spectra $P_1(\omega)$ (*A*) and $P_2(\omega)$ (*B*) for the preferred-condition responses of the V1 simple cell in Fig. 2. In this and subsequent phase plots, phases are plotted in units of π radians. Each phase value is plotted twice to allow for a continuous representation of phases around the circle. Phase coherence is apparent from the appearance of relatively straight line clusters of values for the phase of each $P_n(\omega)$ component. Phase coherence also can be quantified by the Rayleigh Phase Criterion (RPC) (Mardia 1972). For these data, the RPC indicates highly consistent phases ($P <$ 0.001). Less coherence (more scatter of the phases) is noted in the ~22- to 32-Hz range in $P_2(\omega)$ plot. This likely reflects statistical fluctuations because there is no peak in the spectra at this range to suggest a new component in the residual activity.

cycle (1.06 Hz). For the blank condition (Fig. 2*C, bottom*), the "true" value of $P_n(\omega)$ must be zero (for $n > 0$), and thus the measured $P_1(\omega)$ is an indicator of the uncertainty of the statistical estimate. In this cell, for the nonpreferred stimulus, the estimated $P_1(\omega)$ (*middle*) is no different from the estimate obtained in the blank condition. However, for the preferred stimulus (*top*), $P_1(\omega)$ is again approximately threefold higher than in the blank condition, indicating that much of the residual power waxes and wanes with the stimulus cycle, as in Fig. 1, *B* and *C*. Analogously, $P_2(\omega)$ describes the components of the residual activity that are modulated at the second harmonic of the stimulus frequency (Fig. 1*D*). As shown in Fig. 2*D*, the behavior of $P_2(\omega)$ is similar to that of $P_1(\omega)$.

The phase-locked spectral components reveal an aspect of neuronal activity that is distinct from the average response. That is, the average response (the PSTH) is very nearly sinusoidal, but the residual activity is modulated by an envelope that is not sinusoidal [i.e., not confined just to $P_0(\omega)$ and $P_1(\omega)$]. The spectral distribution of the residual activity (the carrier) is indicated by the dependence of $P_1(\omega)$ on ω and is broadband. If oscillations were present, they would be manifest in a narrowband dependence on ω.

The phases of $P_n(\omega)$ for this simple cell (Fig. 3, *A* and *B*)

form relatively straight-line clusters of values, more so for $n = 1$ than for $n = 2$. This supports the interpretation of $P_n(\omega)$ as modulation of the residual activity by a common envelope because the phases of $P_n(\omega)$ (which indicate the phase of the envelope at each frequency) are coherent over the range of frequencies present in the modulated residual activity.

Phase coherence for $P_n(\omega)$ up to the $n = 2$ to $n = 4$ was typical of the data set as a whole (21 cells). However, five cells showed modulation of the residual activity up to at least the $n = 6$ harmonic (the highest harmonic routinely analyzed). The presence of phase coherence of the carriers up to high harmonics of the stimulus cycle indicates that the envelope of the residual activity has rapidly varying components. That is, the residual activity is sharply gated by the periodic stimulus.

Estimation of the envelope

Figure 1, *B–D*, provides examples of signals in which the phase-locked spectra are nonzero only for $n = 0$ and one other low value; in these simple cases, the envelope of the residual activity is a sinusoid. In our data, $P_n(\omega)$ is nonzero for many values of n; this indicates that the envelope of the residual activity is not sinusoidal. Because the phases of $P_n(\omega)$ are approximately coherent over a broad range of carrier frequencies for a given n (Fig. 3), we make the approximation that the residual activity within each frequency range rises and falls at the same time over the stimulus cycle. This allows us to combine the individual values of $P_n(\omega)$ across a range of carriers (ω_{lo} to ω_{hi}), to obtain a more reliable quantity $P_n^{average}$, that represents the nth harmonic of the (assumed) common envelope

$$P_n^{average} = \frac{1}{\omega_{hi} - \omega_{lo}} \int_{\omega_{lo}}^{\omega_{hi}} P_n(\omega) d\omega \qquad (2)$$

We calculate this average as a finite sum over the range 10–50 Hz. The envelope, $E(t)$, is now reconstructed by Fourier synthesis based on $P_n^{average}$

$$E(t) = \sum_n e^{2\pi i nt/S} P_n^{average} \qquad (3)$$

In this reconstruction, we sum over all the n's for which the RPC indicates significance. examined at least up to $n = 6$. The reconstructed envelope (Fig. 4) for the preferred response in this cell resembles the averaged response as seen in the PSTH (Fig. 2*A*) but is less sinusoidal. Moreover, if noise was additive, contributions from $n > 0$ would be equal to 0 and the reconstructed envelope $E(t)$ would be flat (corresponding to the case illustrated in Fig. 1*A*).

Nonpreferred responses in single-unit recordings

In most datasets, residual activity was most prominent for the preferred responses, as illustrated in Fig. 2. Figure 5*A* displays data from a complex cell that shows an atypical response to a nonpreferred grating. The PSTH (Fig. 5*A*) shows a maintained discharge during the presentation of the orthogonal grating and the blank, and modest overall elevation of the mean rate for the preferred condition. $P_0(\omega)$ (Fig. 5*B*) is decreased in the orthogonal condition relative to the preferred and blank conditions. However, the higher-order spectra ($n = 1, 2$) for the orthogonal condition demonstrate the appearance of a
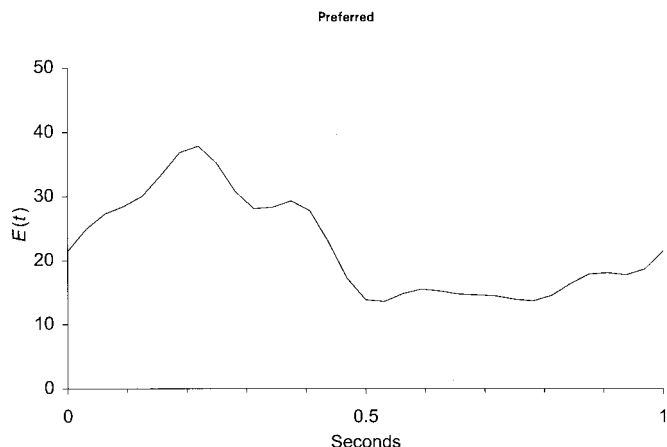
FIG. 4. Reconstructed envelope $E(t)$ that gates the residual activity of the V1 simple cell in the preferred condition illustrated in Fig. 2. $E(t)$ describes the fluctuations of variance as a function of time into the stimulus cycle and has units corresponding to that of $P_n(\omega)$, namely (impulses/s)^2/Hz.

distinct "hump" in the low-frequency range (1–10 Hz) that is not evident in the other conditions (Fig. 5, C and D). The low-frequency hump also is seen in higher-order phase-locked spectra (Fig. 5E), and phase coherence in the 10- to 50-Hz range is observed up to $n = 10$ (data not shown).

The reconstructed envelope for the preferred response (Fig. 6A) is similar to the PSTH of the preferred response (Fig. 5A). This contrasts with the reconstructed envelope for the orthogonal response (Fig. 6B), which has a greater amount of rapid variations than the preferred-response envelope. This indicates sharp gating of the residual activity during the presentation of the orthogonal stimulus. This gating is not evident in the orthogonal-response PSTH, which is minimally different from the PSTH recorded in the blank condition (Fig. 5A).

The strong modulation of residual activity in this case shows that the cell is receiving inputs from other orientations. However, this cross-orientation interaction does not change the average response, but rather consists of peaks of variability at specific times (Fig. 6B) of the stimulus cycle. Another (simple) cell recorded without a blank condition demonstrated a similar phenomenon (sharper gating of the residual activity of the response to a nonpreferred grating compared with the response to a preferred grating). That is, these two units showed evidence of a novel aspect of cross-orientation interaction: a modulation in the residual activity with little or no modulation in the average response.

Simultaneous MUAs and SUAs

In the datasets with simultaneous recordings of SUA pairs and MUA, we examined not only the phase-locked spectra within channels but also the phase-locked cross-spectra. As detailed in the APPENDIX, the phase-locked cross-spectra describe how cross-covariances between channels vary throughout the stimulus cycle. We use $P_{n;j,k}(\omega)$ to denote the phase-locked cross-spectrum of order n between channels j and k. $P_{n,j}(\omega)$ denotes the phase-locked spectrum of order n on channel j considered in isolation.

Figure 7, A–C, shows phase-locked spectra and cross-spectra for two cells recorded simultaneously from electrodes 2 mm displaced (laterally) in parafoveal V1. Channel $j = 1$ is a simple cell, and channel $j = 2$ is a complex cell. For a drifting grating at a preferred orientation, the simple cell's PSTH showed a strongly modulated response and the complex cell's PSTH showed an elevation of maintained discharge. In both single units, phase coherence was strong for $P_{1;j}(\omega)$ and obvious but weaker for $P_{2;j}(\omega)$ (Fig. 7, A and B). The RPC statistic showed statistically significant coherence for $n = 1, 2, 3,$ and 5 in both units. Figure 7C shows the phase-locked cross-spectra, $P_{n;1,2}(\omega)$ for $n = 0, 1,$ and 2. For $n = 0$, there is phase-coherence, indicating correlated activity between the two recorded units. [The Fourier transform of this spectrum, essentially the shuffle-corrected cross-correlogram, shows that this cross-correlation is maximal at 0 time lag, as would be expected from the clustering of the phases of $P_{0;1,2}(\omega)$ around 0]. The phase-locked cross-spectrum, $P_{n;1,2}(\omega)$ for $n > 0$, measures the component of this correlation that varies with the nth harmonic of the stimulus cycle. As can be seen in Fig. 7C, the amplitudes are lower than that of $P_{0;1,2}(\omega)$, and there is little, if any, phase coherence. The finding of a reduction or loss of phase coherence in the phase-locked cross-spectra (compared with individual phase-locked spectra) was typical of SUA/SUA recordings from independent electrodes. It indicates that although the residual activity on the two channels is correlated ($n = 0$), this correlation is not detectably gated by the stimulus. The reconstructed envelopes for each single unit and the cross-spectra are displayed in Fig. 8, A–C. The envelope of the cross-spectra (Fig. 8C) is lower in amplitude than that of either single unit (A or B).

For the three pairs (6 cells) recorded in SUA pairs, common gating of residual activity was weaker than gating of residual activity in individual units. As in this case, some common gating was observed, but the cross-spectral residual components were never as prominent as those seen in either individual unit. Correlations of individual SUA and MUA were also typically independent of the stimulus, even though individual SUA and MUA residual activities were strongly modulated by the stimulus, up to the $n = 5$ or $n = 6$ harmonic of the stimulus cycle. In five SUA/MUA recordings from the same electrode, the cross-spectra $P_{n;1,2}(\omega)$ ($n > 0$) were insignificant even though analysis of individual channels [$P_{n;1}(\omega)$ and $P_{n;2}(\omega)$] revealed modulation of the residual activity. In a similar analysis for another pair recording of two complex cells ($j = 1, 2$), recorded from two electrodes during stimulation with a preferred drifting grating at a low spatial frequency of 0.25 cycles/°, but not others at higher spatial frequencies, both cells exhibited very strong gating by the stimulus.

Some recordings also showed a narrow band of activity consistent with oscillations superimposed on the broadband activity that was universally observed. Figure 9 shows the phase-locked spectrum $P_{n;1}(\omega)$ ($n = 0, 1, 2$) of the simple cell shown in Fig. 7A plotted on a linear scale to emphasize this narrowband activity at ~10 Hz (thin arrows). This peak is present for $n > 0$, but less distinct, indicating that the oscillatory activity was only partially gated by the stimulus cycle. In addition, a broader hump, spanning ~15 Hz (thick arrows) between carrier frequencies 20–35 Hz, is present up to at least $n = 4$ (only $n = 1, 2$ shown), indicating nonoscillatory activity in the same frequency range is gated by the stimulus. The second single unit in this recording did not show the sharp peak at 10 Hz, but did show a slight "hump" for $n = 1$ in the 20- to 35-Hz range of frequencies.
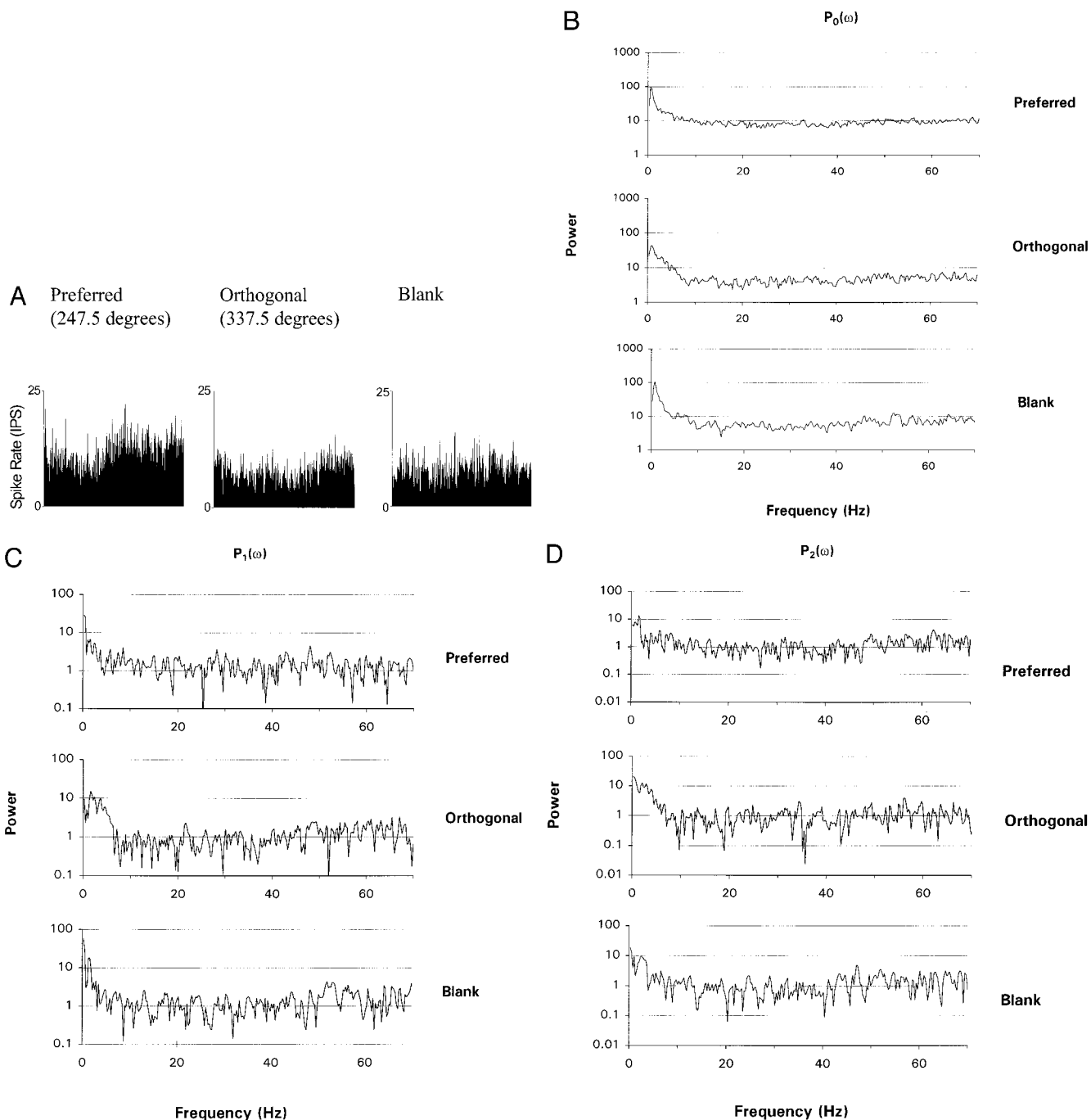
FIG. 5. *A*: peristimulus histograms of a V1 complex cell's response to drifting gratings presented at an orientations of 247.5° (preferred) or 337.5° (orthogonal), spatial frequency of 2 cycles/°, temporal frequency of 1.06 Hz and 100% contrast, and a blank condition (0% contrast). There is an an elevation of the mean rate for the prefered condition and a maintained discharge during the blank and orthogonal conditions. *B*: power spectrum $P_0(\omega)$ corrected for the driven response. There is a decrease in power in the orthogonal condition compared with the preferred and blank conditions. *C*: amplitude of the first-order phase-locked spectrum $P_1(\omega)$. There is a distinct "hump" in the low-frequency range (1–10 Hz) primarily in the orthogonal condition. *D*: amplitude of the second-order phase-locked spectrum $P_2(\omega)$. *E*: phase (*left*) and amplitude (*right*) of the first 5 phase-locked spectra (amplitude for $n = 1$ reproduced from *C*; amplitude for $n = 2$ reproduced from *D*). Presence of phase coherence in the high-order spectra indicates that the residual activity is sharply gated by the periodic stimulus.

DISCUSSION

Summary of results

Stimulus-dependent spectral components in the residual activity were identified using PLSA in single-unit responses of 21 macaque V1 cells. In most of the cells, we found that residual

activity was gated by the stimulus during presentation of a periodic drifting grating. This gating was not merely a "side effect" of modulation of the average firing rate: in many cases, modulation was present up to the $n = 6$ harmonic of the stimulus cycle, even though the stimulus induced either a
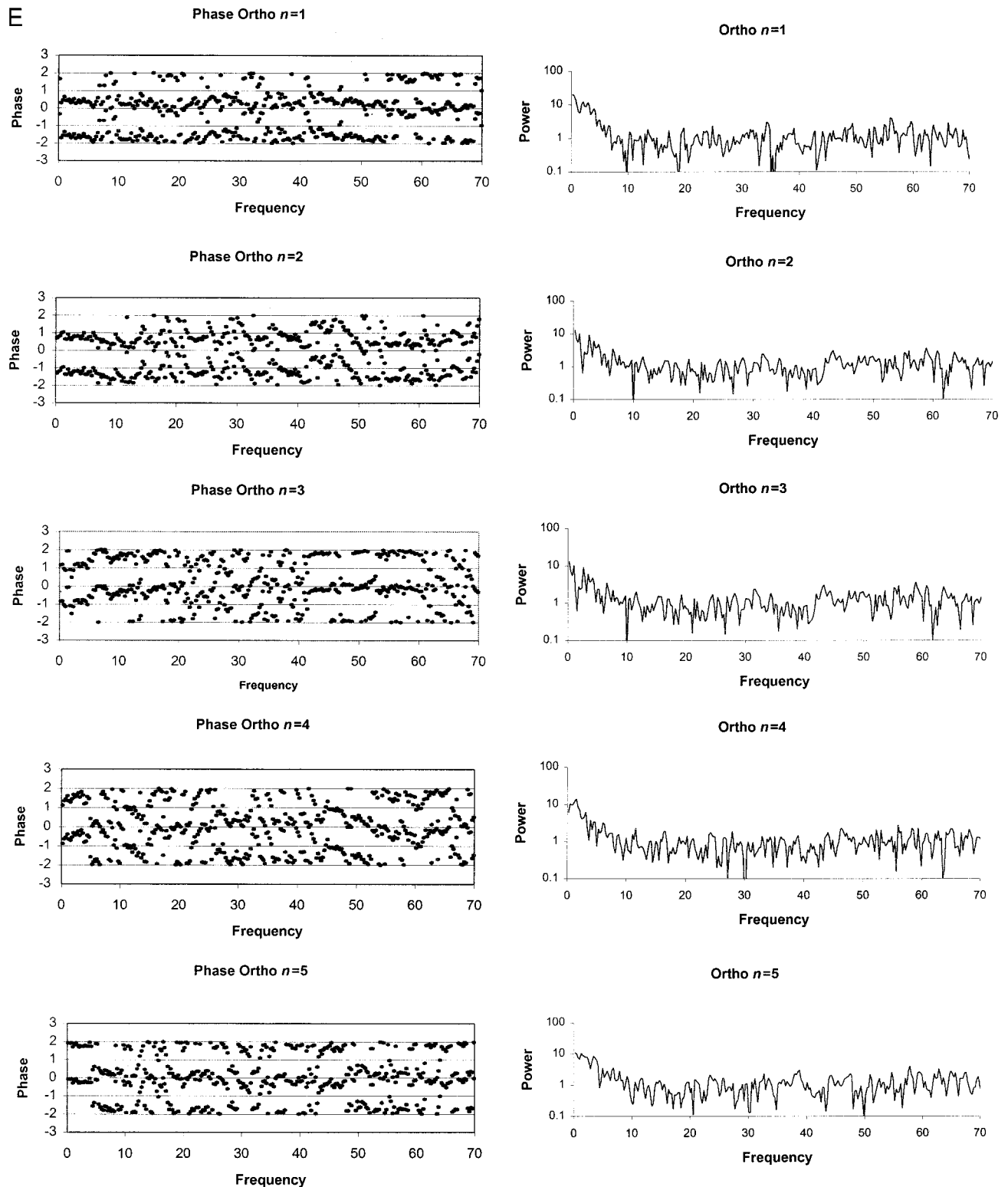
FIG. 5. (continued)

nearly sinusoidal average response (PSTH) or primarily an elevation of the maintained discharge. Furthermore, two cells showed gating of the residual activity during the presentation of a nonpreferred stimulus, thus indicating a novel form of cross-orientation interactions. These SUA recordings from ma-

caque V1 are consistent with previously identified PLSA components in local field potentials from this region (Victor et al. 1993). Oscillations were only occasionally seen in the average power spectra $P_0(\omega)$ of individual single units. In this regard, it may be important that all recordings were done with sufentanil
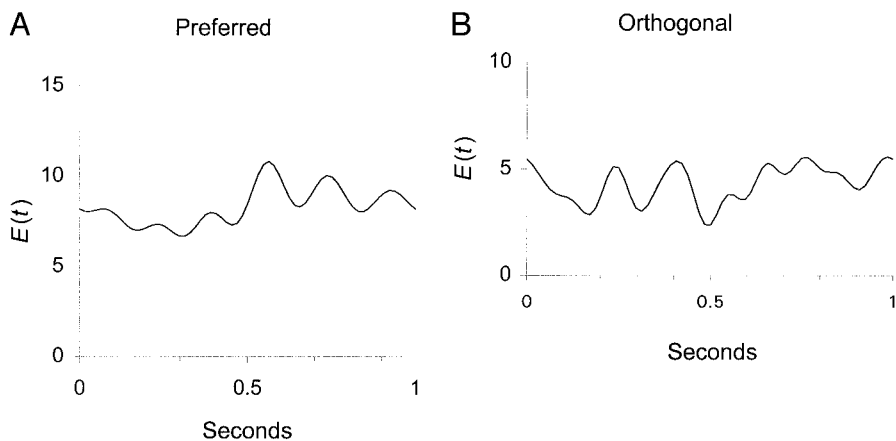
FIG. 6. Reconstructed envelopes $E(t)$ that gate the residual activity of the V1 complex cell of Fig. 5, for the preferred condition (A) and the orthogonal condition (B).

anesthesia in light of recent evidence that opiate anesthetics may block high-frequency oscillations in the gamma range (Whittington et al. 1998).

In six cells, cross-spectra derived from SUA/SUA pair recordings revealed that gating of the residual activity of individual units by the stimulus typically was reduced (or in some cases eliminated) in the phase-locked cross-spectra. Similar results were seen in 11 SUA/MUA pairs. While some single-unit pairs did demonstrate strong gating of their covariances, this was true only for selective stimulus parameters. The decrease in phase-locked residual activity in the cross-spectra of both SUA/SUA and SUA/MUA recordings suggests that envelopes of residual activity seen in different individual single units gate substantially independent sources of ongoing activity. Furthermore, the appearance of joint modulation for certain stimulus parameters but not others suggests that the common gating reflects dynamic changes in functional connectivity rather than hard wiring (Vaadia et al. 1995).

Mean-variance relationship

Previous workers also have noted that the variability of cortical neurons is stimulus dependent and depends on the mean firing rate (Tolhurst et al. 1983). This mean-variance relationship predicts that the residual activity is nonzero but does not by itself predict the form of the residual activity because it does not model the dynamics of the dependence. One way to compare the mean-variance relationship to our analysis is to hypothesize that the variance depends on the instantaneous (expected) mean firing rate and that the variance at nearby times is independent. Under this hypothesis, the phase-locked spectra $P_n(\omega)$ are predicted to be independent of the carrier frequency ω, and the synthesized envelope will be a scaled replica of the average response histogram (adjusted by the windowing function). Thus the mean-variance relationship accounts for the shape of the synthesized envelope observed in most units. It also could account for our observations that phase-locked cross-spectra between units tend to be small, if the variability in the two units' responses are independently related to their means. However, the mean-variance relationship, along with these simple dynamics, does not account for the dependence of the phase-locked spectra $P_n(\omega)$ on ω. This dependence requires that variability at distinct times are correlated—the phase-locked spectra represent the Fourier transform of this autocorrelation structure. This mean-variance re-

lationship also does not account for the behavior of the few units in which the phase-locked spectra are prominent for stimuli that do not change the mean firing rate or for the sharp gating of the envelopes that also are seen occasionally (e.g., Fig. 6B). These observations appear to require a separate source of variability not directly related to the average response.

Comparison of PLSA with related methods

Several methods of signal analysis share a common goal of a search for an interaction between autonomous and stimulus-driven activity. These techniques all examine second-order statistics of signals and have as their null hypothesis that trial-to-trial variability can be explained by stimulus-independent additive noise. In each analysis, the residual activity may be considered to be a carrier, and its possible interaction with the stimulus is considered to be described by a window of modulation (envelope). The distinction between these methods is whether carrier and envelope are viewed in the time domain or in the frequency domain and whether or not a periodic or transient event may interact with the signal.

To make these similarities more explicit, we introduce a new quantity $B(t, \tau)$, closely related to the shuffle-corrected cross-correlogram, a well-known technique for analyzing spike trains (Perkel et al. 1967). We call this function as the "time-resolved autocorrelogram" and define it formally as

$$B(t, \tau) = \left\langle \left(s\left(t + \frac{\tau}{2}\right) - \left\langle s\left(t + \frac{\tau}{2}\right) \right\rangle \right) \left(s\left(t - \frac{\tau}{2}\right) - \left\langle s\left(t - \frac{\tau}{2}\right) \right\rangle \right) \right\rangle \quad (4)$$

Here $\langle \ \rangle$ indicates an average across independent samples of data taken at the same time t following a repetitive transient or initial phase of a stimulus cycle. In essence $B(t, \tau)$ is similar to the signal's autocorrelation (with lag τ), but it is specific to the time t following the reference mark and has been corrected for the average response modulation. $B(t, \tau)$ can be viewed as a joint-PSTH (Aertsen et al. 1989), in which the same neuron's response is collected on both channels and the mean response is subtracted. The null hypothesis that signal and noise do not interact corresponds to the statement that $B(t, \tau)$ is independent of t and also independent of the presence of the stimulus.

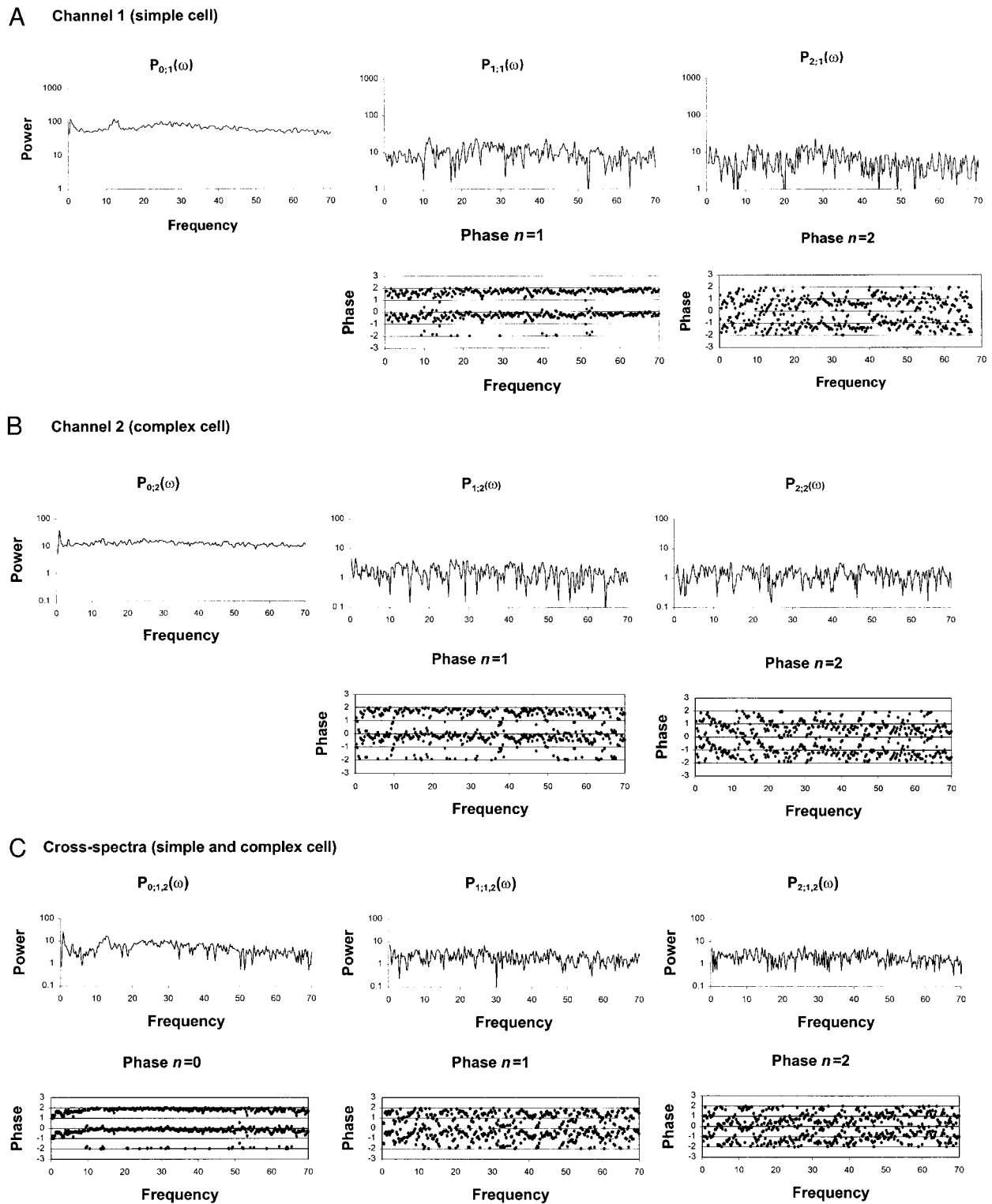Figure 10 displays the connection between different analytic

FIG. 7. Phase-locked spectra and cross-spectra for a simple and a complex cell recorded simultaneously from electrodes 2 mm displaced (laterally) in parafoveal V1. Stimulus was a preferred drifting grating, at an orientation of 45°, a spatial frequency of 2 cycles/°, a temporal frequency of 1.06 Hz and 50% contrast. For these parameters, the simple cell showed a strongly modulated response and the complex cell showed an elevation of maintained discharge (not shown). A and B: amplitudes (top) and phases (bottom) of the single-channel phase-locked spectra $P_{n;j}(\omega)$ for the simple cell ($j = 1$, A) and the complex cell ($j = 2$, B), for orders $n = 0$, 1, and 2. [Phases for $P_{0j}(\omega)$ are forced to be 0, and are not shown]. In both single units, strong phase coherence for $P_1(\omega)$ was present. C: amplitudes and phases of the phase-locked cross-spectra $P_{n;1,2}(\omega)$ for these units. For $n = 0$, there is phase coherence, indicating correlated activity between the 2 recorded units.
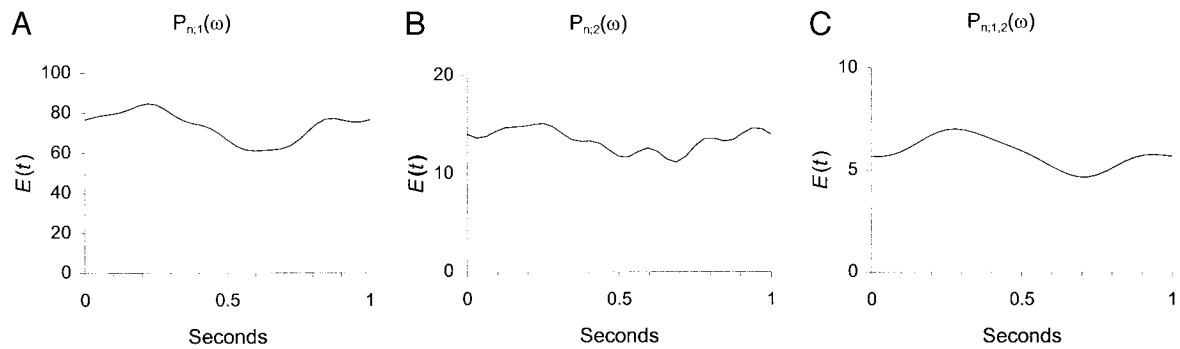
FIG. 8. Reconstructed envelopes $E(t)$ that gate the residual activity of the V1 cells of Fig. 7. A: simple cell; B: complex cell; C: cross-covariance. Note the differing vertical scales between panels.

techniques in the family that includes PLSA. $B(t, \tau)$, when averaged over the stimulus cycle to remove the dependence on t, is the shuffle-corrected autocorrelogram, $\mathrm{SAC}(\tau)$:

$$\frac{1}{S} \int_0^S B(t, \tau) \mathrm{dt} = \mathrm{SAC}(\tau) \qquad (5)$$

FIG. 9. Amplitudes of the phase-locked spectra $P_{n;1}(\omega)$ ($n = 0, 1, 2$) of the 1st cell in Fig. 7 replotted on a linear scale to emphasize a narrowband of oscillatory activity at ~10 Hz (thin arrows). This narrow peak is present for $n > 0$, indicating that the oscillatory activity was gated by the stimulus cycle. In addition, a broader hump, spanning ~10 Hz (thick arrows), is present up to at least $n = 4$ (only $n = 1, 2$ shown), indicating that less sharply tuned activity in the same frequency range also is gated by the stimulus.

The SAC is a special case of the Fourier transform of $B(t, \tau)$ with respect to the *envelope* variable t. The more general quantity is the phase-locked autocorrelation function $A_n(\tau)$

$$\frac{1}{S} \int_0^S e^{(-2\pi i n t)/S} B(t, \tau) \mathrm{dt} = A_n(\tau) \qquad (6)$$

This quantity $A_n(\tau)$ is the component of autocorrelation that varies with the *n*th harmonic of stimulus period. For $n = 0$, $A_n(\tau)$ is the shuffle-corrected autocorrelogram.

A second Fourier transformation, this time in the carrier variable τ, transforms $A_n(\tau)$ into $P_n(\omega)$. This transformation makes sense if the stimulus S is periodic. That is, for a periodic stimulus, the time-resolved autocorrelogram $B(t, \tau)$ is related to $P_n(\omega)$ by a double Fourier transform

$$P_n(\omega) = \frac{1}{S} \int_0^S \int_{-\infty}^{\infty} e^{(-2\pi i n t)/S} e^{-i\omega\tau} B(t, \tau) \mathrm{dt} \mathrm{d}\tau \qquad (7)$$

Another method in this family is time-frequency analysis (Tallon-Baudry et al. 1996). In this method, the envelope is described in the time domain and the carrier is described in the frequency domain. As seen in Fig. 10, the key quantity, $Q(t, \omega)$ can be obtained either by Fourier transformation of the carrier variable τ of the time-resolved cross-correlation $B(t, \tau)$ or by Fourier transformation of the envelope variable ω of the phase-locked spectrum:

$$Q(t, \omega) = \sum_n e^{(2\pi i n t)/S} P_n(\omega) = \int_{-\infty}^{\infty} e^{-i\omega\tau} B(t, \tau) \mathrm{d}\tau \qquad (8)$$

This quantity generalizes $E(t)$ (see *Eq. 3*) by relaxing the constraint that all frequencies are modulated by the same envelope (i.e., the carriers are allowed to have different phases). $E(t)$ can be recovered from $Q(t, \omega)$ by averaging over frequencies (see *Eqs. 2* and *3*). $Q(t, \omega)$ is essentially the Wigner transform of the second-order statistics of the signal. While the Wigner transform does not offer an optimal time-frequency decomposition, improved estimates can be obtained by windowing techniques (see Mitra and Pesaren 1999).

The above paragraphs provide for a common framework to discuss several, apparently quite diverse, investigations. In each case, properties of the residual activity are analyzed by one of the above techniques, depending on the nature of the stimulus signal (periodic or transient) and on whether the phenomena of interest are best described in the time or frequency domain. For example, Vaadia and colleagues (1995)
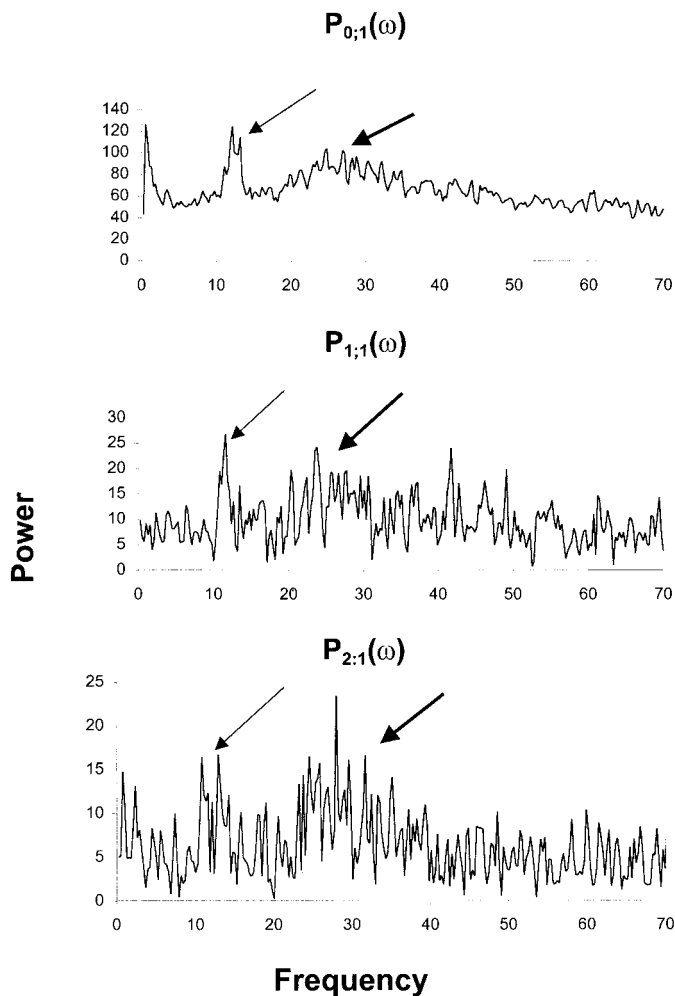
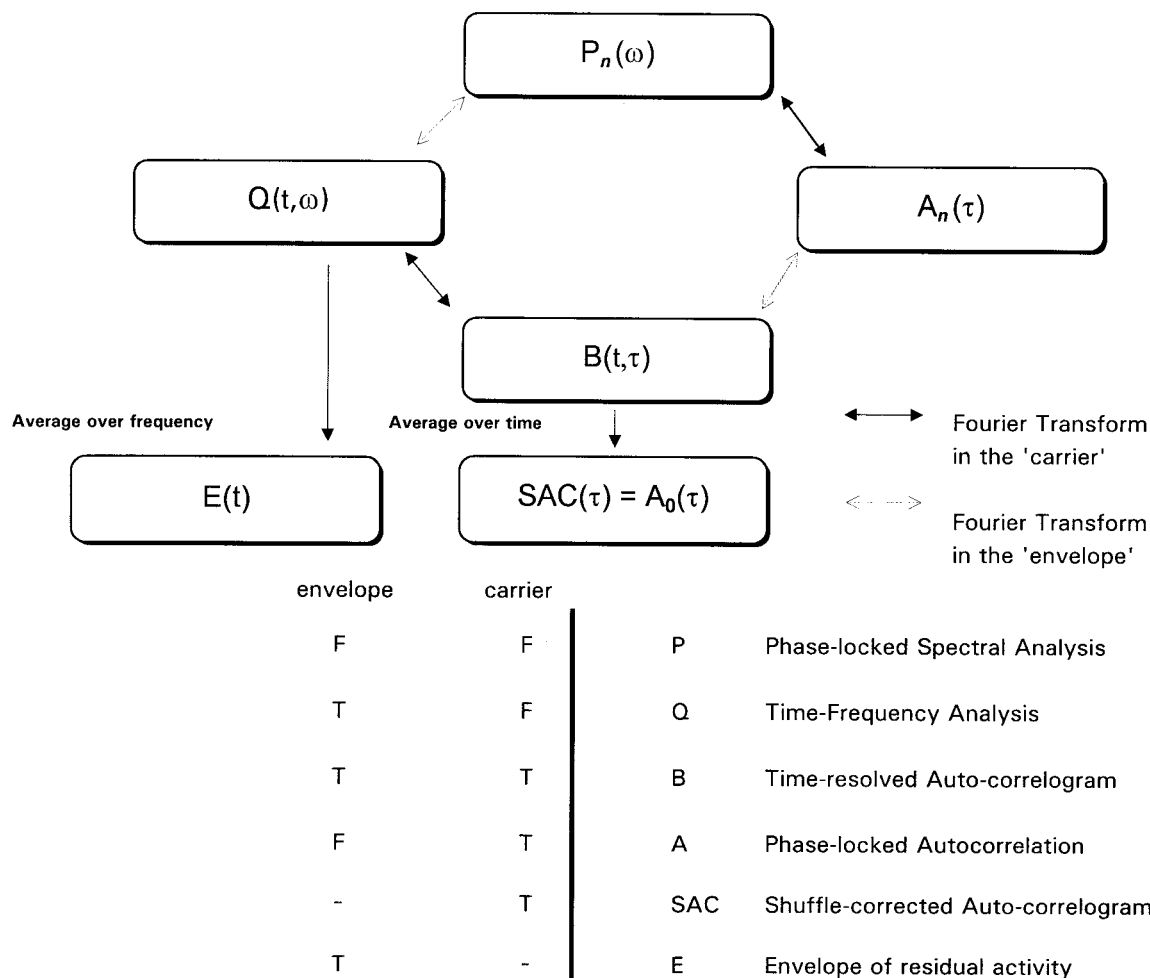| envelope	carrier		
F	F	P	Phase-locked Spectral Analysis
T	F	Q	Time-Frequency Analysis
T	T	B	Time-resolved Auto-correlogram
F	T	A	Phase-locked Autocorrelation
–	T	SAC	Shuffle-corrected Auto-correlogram
T	–	E	Envelope of residual activity

FIG. 10. Relationship of several different approaches to the analysis of residual activity. Solid arrows represent Fourier transformation in the carrier variable; dotted arrows represent Fourier transformation in the envelope variable.

examined multiple single neuron responses during the performance of a GO/NO-GO paradigm with the joint peristimulus time histogram, JPSTH (see *Eq. 4* and surrounding discussion). These studies demonstrated that dynamic patterns of correlation (without modulation of the mean firing rate) could identify different behavioral responses based on the appearance of the patterned activity in time referenced to the behavioral event. Friston (1995) carefully examined this result and further suggested that changes in correlation may reflect neuronal excitation due to transient responses. This conclusion was reached by principal components analysis of a matrix derived from the JPSTH. Other approaches to the analysis of contributions to the JPSTH based on second-order statistics recently have been developed by Brody (1998) and allow for a separation of contributions of circuit properties and intrinsic membrane properties under certain circumstances.

Heinrich and Bach (1997) calculated $Q(t,\omega)$ from steady-state visual evoked potentials (VEPs) recorded from the human electroencephalogram (EEG) at selected values of ω (30–40 Hz). They labeled these components "residual frequency components." Their temporal envelopes showed that they were stimulus dependent and differed from the standard VEP waveform. Tallon-Baudry and colleagues (1996) analyzed human VEPs obtained during presentations of illusory contour figures. They augmented time-frequency analysis with a wavelet transform to improve frequency and temporal resolution. Their study demonstrated significant non-phased-locked activity in several frequency bands and at different times. Some of the activity in these bands strongly correlated with the perception of an illusory contour.

These studies, which identified interactions of stimulus and residual activity, complement those of Arieli and colleagues (1996). In their study, ongoing brain activity was examined with optical imaging and extracellular recording techniques. Results were interpreted as consistent with linear summation of the deterministic response and the residual activity. However, in this study the high-frequency response was superimposed on slow-frequency components of ongoing activity, or noise. It did not address whether the correlation structure of single-trial responses could in fact be accounted for by the correlation structure measured in the absence of stimulation. In terms of the present study, this approach discards information about $P_n(\omega)$ for $n > 0$ and does not compare $P_0(\omega)$ in stimulus and blank conditions. Thus interactions of the residual activity and the average response were likely to have been overlooked.

Implications for models of brain functions

Several investigators have emphasized the importance of oscillations (Singer and Gray 1995), bursts (Lisman 1997), or

other transient, organized dynamic events in neuronal responses to stimuli (Aertsen et al. 1989; Bullock 1996; Friston 1995, 1997; Victor and Purpura 1996). In striate cortex, oscillations have been described in response to coherent stimuli (Gray 1994). Such activity also has been proposed to reflect formation of neuronal assemblies and to a play a role in linking multiple brain regions and local patches of neuronal circuits to facilitate binding (Llinas et al. 1994; Singer and Gray 1995). These stimulus-dependent events have been postulated to reflect important aspects of brain function other than rate codes. The results here, of residual activity that is strongly modulated by an external stimulus, demonstrate rich spatiotemporal dynamics in neuronal responses. Stimulus-dependent changes in brain activity are not restricted to narrowband, single population phenomena such as oscillations. The envelopes and spectra calculated from PLSA allow us to visualize the dynamics of complex local network inputs that shape individual neuronal responses. Moreover, the diminished stimulus-gated residual activity in cross-spectra, compared with its prominence in individual single-channel phase-locked spectra, suggests that the envelopes of residual activity seen in individual units gate signals from multiple neuronal assemblies with only partial overlap.

APPENDIX: THEORY

Phase-locked spectral analysis

PLSA extends spectral analysis to situations in which a periodic stimulus is present. PLSA is a two-step procedure: estimation of the average response to a periodic stimulus and modified spectral analysis of the residual activity, i.e., the difference between individual responses and the estimated average response. To develop and motivate our method, we begin by revisiting the concepts behind the power spectrum when there is no external stimulus and then extend these concepts to the situation where a periodic stimulus is present. The discussion of the power spectrum is somewhat elaborate, to facilitate an extension to the situation in which a periodic stimulus is present.

No external stimulus

We assume that $s(t)$, the time series to be analyzed, is autonomous and stationary. That is, its statistics are independent of external stimuli and also of our choice of a time t_0 at which to begin the analysis.

Estimation of the power spectrum depends on the statistics of Fourier components obtained from finite segments of the time series $s(t)$. We use $Z(\omega, L, T, t_0)$ to denote the Fourier component at the frequency ω determined from a finite segment of length L that begins after an elapsed time T after the arbitrary start time t_0. Formally

$$Z(\omega, L, T, t_0) = \frac{1}{L}\int_T^{T+L} s(t + t_0)e^{-i\omega t}dt \quad (A1)$$

Changing the elapsed time, T, in (1) by an amount ΔT leads to

$$Z(\omega, L, T + \Delta T, t_0) = \frac{1}{L}\int_{T+\Delta T}^{T+\Delta T+L} s(t + t_0)e^{-i\omega t}dt \quad (A2)$$

The data included in the integral are precisely the same as if the start time t_0 were changed to $t_0 + \Delta T$, but the time to the start of the analysis interval were held fixed at T. With $t' = t - \Delta T$, we find

$$Z(\omega, L, T + \Delta T, t_0) = \frac{1}{L}\int_T^{T+L} s(t' + \Delta T + t_0)e^{-i\omega(t' + \Delta T)}dt'$$

$$= e^{-i\omega\Delta T}\frac{1}{L}\int_T^{T+L} s(t' + t_0 + \Delta T)e^{-i\omega t'}dt' \quad (A3)$$

Thus the numerical values of the Fourier components of *Eq. A2* will be offset with respect to the Fourier components of *Eq. A1* by the phase factor $e^{-i\omega\Delta T}$ in *Eq. A3*

$$Z(\omega, L, T + \Delta T, t_0) = e^{-i\omega\Delta T}Z(\omega, L, T, t_0 + \Delta T) \quad (A4)$$

Autonomy now places strong constraints on the statistics of these Fourier components. First, consider the average of $Z(\omega, L, T, t_0)$ over all integrals of length L (parameterized by the elapsed time, T), which we denote by

$$Z_{av}(\omega, L, t_0) \equiv \langle Z(\omega, L, T, t_0)\rangle_T \quad (A5)$$

Averaging *Eq. A4* over the elapsed time T leads to

$$Z_{av}(\omega, L, t_0) = e^{-i\omega\Delta T}Z_{av}(\omega, L, t_0 + \Delta T) \quad (A6)$$

This must hold for time shift ΔT and frequency ω. On the other hand, because the start time t_0 is arbitrarily chosen, autonomy implies that

$$Z_{av}(\omega, L, t_0) = Z_{av}(\omega, L, t_0 + \Delta T) \quad (A7)$$

Combining *Eqs. A6* and *A7* leads to

$$Z_{av}(\omega, L, t_0)(1 - e^{-i\omega\Delta T}) = 0 \quad (A8)$$

This must hold for all ω and ΔT, so it follows (for $\omega \neq 0$) that $Z_{av}(\omega, L, t_0) = 0$.

Because (as we have just seen) the average values of Fourier components are necessarily 0, we examine the next simplest candidate to characterize the statistics of the Fourier components: their variances and covariances. We denote an averaged covariance of Fourier components at two frequencies ω_1 and ω_2 by

$$X_{av}(\omega_1, \omega_2, L, t_0) \equiv \langle [Z(\omega_1, L, T, t_0) - Z_{av}(\omega_1, L, t_0)][(Z(\omega_2, L, T, t_0)$$
$$- Z_{av}(\omega_2, L, t_0)]\rangle_T \quad (A9)$$

We use $\delta Z(\omega, L, T, t_0)$ to denote a sample of residual activity, namely the departure of a Fourier component obtained from an individual segment from its average value

$$\delta Z(\omega, L, T, t_0) = Z(\omega, L, T, t_0) - Z_{av}(\omega, L, t_0) \quad (A10)$$

Retaining the term $Z_{av}(\omega, L, t_0)$ in *Eq. A10* (even though it is 0 when no external stimulus is present) allows the equation to apply more generally (see following text). *Equation A9*, for the average covariance of the spectral components, takes the form

$$X_{av}(\omega_1, \omega_2, L, t_0) = \langle [\delta Z(\omega_1, L, T, t_0)][\delta Z(\omega_2, L, T, t_0)]\rangle_T \quad (A11)$$

As we now show, for a process in which the starting time t_0 can be chosen arbitrarily, the ordinary power spectrum amounts to a calculation of X_{av}. On the one hand, shifting the start time of the analysis interval from T to $T+\Delta T$ leads to an equation analogous to *Eq. A6*

$$X_{av}(\omega_1, \omega_2, L, t_0) \equiv e^{-i\omega_1\Delta T}e^{-i\omega_2\Delta T}X_{av}(\omega_1, \omega_2, L, t_0 + \Delta T) \quad (A12)$$

On the other hand the assumption of autonomy leads to an equation analogous to *Eq. 7*

$$X_{av}(\omega_1, \omega_2, L, t_0) = X_{av}(\omega_1, \omega_2, L, t_0 + \Delta T) \quad (A13)$$

Combining *Eqs. A12* and A13 leads to

$$X_{av}(\omega_1, \omega_2, L, t_0)(1 - e^{-i(\omega_1 + \omega_2)\Delta T}) = 0 \quad (A14)$$

which must hold for any ΔT. Thus X_{av} must equal zero when $\omega_1 + \omega_2 \neq 0$.

When $\omega_1 + \omega_2 = 0$ in *Eq. A14,* we may choose $\omega_1 = \omega$ and $\omega_2 = -\omega$. *Equation A11* then becomes

$$X_{av}(-\omega, \omega, L, t_0) = \langle \overline{\delta Z(\omega, L, T, t_0)} \delta Z(\omega, L, T, t_0) \rangle_T$$
$$= \langle |\delta Z(\omega, L, T, t_0)|^2 \rangle_T \quad (A15)$$

The right hand side of *Eq. A15* is the variance of Fourier components determined from segments of length L. It therefore is related to the power spectrum $P(\omega)$ (Blackman and Tukey 1959) by

$$P(\omega) = \lim_{L \to \infty} L X_{av}(-\omega, \omega, L, t_0) \quad (A16)$$

Equations A15 and *A16* are independent of the start time t_0, and thus we may choose $t_0 = 0$. $X_{av}(\omega, -\omega, L, 0)$ approaches its asymptotic limit of $P(\omega)/L$ (*Eq. A16*) when L is larger than any correlation times of the signal $s(t)$ (Victor and Mast 1991). Thus in the autonomous case, second-order statistics (*Eq. A9*) of $\delta Z(\omega, L, T, 0)$ are described by the power spectrum: the covariances ($\omega_1 + \omega_2 \neq 0$ in *Eq. A11*) are zero, and the variances ($\omega_1 = -\omega_2$ in *Eq. A11*) are related to the power spectrum by *Eq. A16*.

Periodic external stimulus

When a periodic external stimulus is present, shifting the start time t_0 of the analysis by arbitrary amounts may change the observed statistics, because the stimulus cycle provides a periodic marker (see Fig. 1, *B–D*). However, for a stationary system, shifts of the start time by a multiple of the stimulus period will leave the observed statistics unchanged. We assume that the analysis period L is a multiple of the stimulus period S.

The definition (*Eq. A11*) of the covariance $X_{av}(\omega_1, \omega_2, L, t_0)$ still makes sense, but the average over elapsed time T must be restricted to values of T that are multiples of S to avoid averaging together estimates that begin at different phases of the external stimulus. Furthermore, because the external stimulus provides a time marker with period S, equality in *Eq. A13* only can be guaranteed for shifts ΔT that are integer multiples of S. Thus the relationship *Eq. A14* holds only when ΔT is a multiple of S. It follows that $X_{av}(\omega_1, \omega_2, L, t_0)$ can have nonzero values whenever $\omega_1 + \omega_2 = (2\pi n)/S$, for any integer n (and not just $n = 0$, as in the "no external stimulus" case).

We let $\omega = (-\omega_1 + \omega_2)/2$. The condition for a nonzero covariance, $\omega_1 + \omega_2 = 2\pi n/S$, becomes $\omega_1 = (\pi n/S) - \omega$ and $\omega_2 = (\pi n/S) + \omega$. In analogy with the standard power spectrum (*Eq. A16*), we define the phase-locked spectrum (with start time $t_0=0$) as

$$P_n(\omega) = \lim_{L \to \infty} L X_{av}\left(\frac{\pi n}{S} - \omega, \frac{\pi n}{S} + \omega, L, 0\right). \quad (A17)$$

This quantity describes the second-order statistics (variances and covariances) of $\delta Z(\omega, L, T, 0)$ in the presence of a periodic external stimulus. For $n = 0$, this is the power spectrum of a signal $s(t)$ from which the driven components (the average Fourier components) have been subtracted. The presence of an external stimulus allows the covariance of Fourier components at the frequencies $(\pi n/S) - \omega$ and $(\pi n/S) + \omega$ to be nonzero for $n > 0$, because of the restrictions of values of ΔT in *Eq. A12*.

Note that the condition that time-shift by a stimulus period S leave the observed statistics unchanged explicitly excludes the possibility of period-doubling (Feigenbaum 1983) and other related phenomena. However, our analysis could be generalized to this situation by replacing the stimulus period S by a suitable multiple MS in the formalism in the preceding text.

Phase-locked spectra for multiple-channel recordings

The above procedures may be extended to multichannel data. We use $Z_j(\omega, L, T, t_0)$ to denote the Fourier component at the frequency ω determined from a segment of length L on channel j, beginning at elapsed time T after the arbitrary start time t_0 (*Eq. A19*). In analogy to *Eq. A5*, we use $Z_{j,av}(\omega, L, t_0)$ to represent their average over a set of intervals parameterized by T. The set of covariances of these components includes not only cross-products within a channel j but also between pairs of channels j and k. Thus for multichannel data, the definition of the cross-covariances, analogous to *Eq. A9,* is

$$X_{av;j,k}(\omega_1, \omega_2, L, t_0) \equiv \langle [Z_j(\omega_1, L, T, t_0) - Z_{j,av}(\omega_1, L, t_0)][(Z_k(\omega_2, L, T, t_0)$$
$$- Z_{k,av}(\omega_2, L, t_0)] \rangle_T \quad (A18)$$

The phase-locked *cross-spectrum*, $P_{n;j,k}$, is defined by

$$P_{n;j,k}(\omega) = \lim_{L \to \infty} L X_{av;j,k}\left(\frac{\pi n}{S} - \omega, \frac{\pi n}{S} + \omega, L, 0\right) \quad (A19)$$

$P_{n;j,k}(\omega)$ indicates the extent to which the cross-spectra of the residual activity in channels j and k fluctuate with the nth harmonic of the stimulus cycle. If these residuals were uncorrelated, then $P_{n;j,k}(\omega)$ would be 0 for all values of n. If these residuals were correlated but did not wax and wane with the stimulus cycle, then $P_{n;j,k}(\omega)$ would be 0 for $n > 0$, and $P_{0;j,k}(\omega)$ would be the Fourier transform of the shuffle-corrected cross-correlogram between channels j and k (see DISCUSSION).

Note (from *Eqs. A18* and *19*) that the phase of the cross-spectrum is the combined result of two influences. One contribution, analogous to the phase of the single-channel phase-locked spectrum, is the phase of the modulation envelope. This contribution is independent of ω. The second contribution is specific to the multichannel situation and arises if there is a phase difference of the carriers on the two correlated channels. If, for example, the residual activity on two channels is correlated with a delay τ between channel 1 and channel 2 (channel 1 earlier than channel 2), then this delay contributes a phase of $e^{-i\omega\tau}$ to $P_{0;1,2}(\omega)$. Phase coherence remains a valid test for the significance of $P_{n;j,k}(\omega)$. A band of consistent phases indicates a band of frequencies in which the residual activity on two channels is correlated at particular times in the stimulus cycle (the 1st contribution). A nonzero slope of the phases within this band indicates a temporal shift of the carriers between the channels (the second contribution).

REFERENCES

ABELES, M. AND GERSTEIN, G. L. Detecting spatiotemporal firing patterns among simultaneously recorded single neurons. *J. Neurophysiol.* 60: 909–924, 1988.

AERTSEN, A., GERSTEIN, G., HABIB, M., AND PALM, G. Dynamic of neuronal firing correlation: modulation of 'effective connectivity'. *J. Neurophysiol.* 61: 900–917, 1989.

ARIELI, A., STERKIN, A, GRINVALD, S., AND AERSTEN, A. Dynamics of ongoing activity: explanation of the large variability in evoked cortical responses. *Science* 273: 1868–1871, 1996

BLACKMAN, R. AND TUKEY, J. *The Measurement of Power Spectra.* New York: Dover Books, 1959

BRODY, C. D. Slow covariations in neuronal resting potentials can lead to artefactually fast cross-correlations in their spike trains. *J. Neurophysiol.* 80: 3345–3351, 1998.

BULLOCK, T. Signals and signs in the nervous system: the dynamic anatomy of electrical activity is probably information rich. *Proc. Natl. Acad Sci. USA* 94: 1–6, 1996

FEIGENBAUM, M. Universal behavior in nonlinear systems. *Physica.* 7: 16–39, 1983.

FREEMAN, W. AND BARRIE, J. M. Chaotic oscillations and the genesis of meaning in cerebral cortex. In: *Temporal Coding in the Brain,* edited by G. Buzsaki. Berlin: Springer-Verlag, 1994.

FRISTON, K. Neuronal transients. *Proc. R. Soc. Lond. B Biol. Sci.* 261: 401–405, 1995

FRISTON, K. Another neural code? *Neuroimage* 5: 213–220, 1997.

GERSHON, E. D., WIENER, M. C., LATHAM, P. E., AND RICHMOND, B. J. Coding strategies in monkey V1 and inferior temporal cortices. *J. Neurophysiol.* 79: 1135–1144, 1998

GRAY, C. Synchronous oscillations in neuronal systems: mechanisms and functions. *J. Computat. Neurosci.* 1: 11–38, 1994

HEINRICH, S. P. AND BACH, M. Stimulus-induced modulations of 30 and 40 Hz domains in the EEG. *Abstract ARVO.* 4618-B125, 1997

LISMAN, J. Bursts as a unit of neural information: making unreliable synapses reliable. *Trends Neurosci.* 20: 38–43, 1997.

LLINAS, R., RIBARY, U., JOLIOT, M., AND WANG, X. J. Context and content in temporal thalamocortical binding. In: *Temporal Coding in the Brain,* edited by G. Buzsaki. Berlin: Springer, 1994.

MARDIA, K. V. *Statistics of Directional Data.* New York: Academic, 1972.

MITRA, P. P. AND PESARAN, B. Analysis of dynamic brain imaging data. *Biophys. J.* 76: 691–708, 1999.

MORAN, J. AND DESIMONE, R. Selective attention gates visual processing in the extrastriate cortex. *Science* 229: 782–784, 1985.

PERKEL, D., GERSTEIN, G., AND MOORE, G. Neuronal spike trains and stochastic point processes. *Biophys. J.* 391–418: 1967.

SINGER, W. AND GRAY, C. Visual feature integration and the temporal correlation hypothesis. *Annu. Rev. Physiol.* 55: 349–374, 1995.

SKOTTUN, B. C., DE VALOIS, R. L., GROSOF, D. H., MOVSHON, J. A., ALBRECHT, D. G., AND BONDS, A. B. Classifying simple and complex cells on the basis of response modulation. *Vision Res.* 31: 1078–1086, 1991.

TALLON-BAUDRY, C., BERTRAND, O., DELPUECH, C., AND PERNIER, J. Stimulus specificity of phase-locked and non-phase-locked 40 Hz visual responses in human. *J. Neurosci.* 16: 4240–4249, 1996.

TOLHURST, D. J., MOVSHON, J. A., AND DEAN, A. F. The statistical reliability of signals in single neurons in cat and monkey visual cortex. *Vision Res.* 23: 775–785, 1983

TREUE, S. AND MAUNSELL, J.H.R. Attentional modulation of visual motion processing in cortical areas MT and MST. *Nature* 382: 539–541, 1996.

VAADIA, E., HAALMAN, I, ABELES, M., BERGMAN, H., PRUT, Y., SLOVIN, H., AND AERTSEN, A. Dynamics of neuronal interactions in monkey cortex in relation to behavioural events. *Nature* 373: 515–518, 1995.

VICTOR, J. D, CANEL, A., AND PURPURA, K. P. Stimulus-dependent changes in the correlation structure of the activity of neuronal populations in primary visual cortex of macaque. *Abstr. Soc. Neurosci.* 1574, 1993.

VICTOR, J. D. AND MAST, J. A new statistic for steady-state evoked potentials. *Electroencephalogr. Clin. Neurophysiol.* 78: 378–388, 1991.

VICTOR, J. D. AND PURPURA, K. P. Nature and precision of temporal coding in visual cortex: a metric space analysis. *J. Neurophysiol.* 76: 1310–1326, 1996.

VICTOR, J. D. AND PURPURA, K. P. Spatial phase and the temporal structure of the response to gratings in V1. *J. Neurophysiol.* 80: 554–571, 1998.

VICTOR, J. D., PURPURA, K. P., KATZ, E., AND MAO, B. Population encoding of spatial frequency, orientation, and color in macaque V1. *J. Neurophysiol.* 72: 2151–2166, 1994.

WHITTINGTON, M. A., TRAUB, R. D., FAULKNER, H. J., JEFFERYS, J.G.R., AND CHETTIAR, K. Morphine disrupts long-range synchrony of gamma oscillations in hippocampal slices. *Proc. Natl. Acad. Sci. USA* 95: 5807–5811, 1998.